2022 DTC Visitor Program Final Report

UFS METplus Hack-A-Thon[1]

Implementation of MJO-ENSO Diagnostics for Seasonal Forecasts in METplus

Cristiana Stan[2] and Loren Doyle

George Mason University

DTC Host: Tara Jensen

[1] Due to insufficient interest from graduate students in participating in the hack-a-thon, the original project was rescoped without changing the original goal of increasing student engagement and experience with METplus.
[2] cstan@gmu.edu

Introduction

The demand for climate models to be used for seamless prediction from a few days to multi-decades is challenging the representation of coupling between the components of the climate system. One example is the time scale interactions between the fast-evolving modes of atmospheric variability and slowly-varying oceanic modes in the tropical Pacific. Climate variability in the tropical Pacific is dominated by two phenomena: El Niño – Southern Oscillation (ENSO) on interannual (2 to 7 years) timescales and tropical oscillations on intraseasonal (20 to 120 days) timescales. ENSO variability occurs primarily in the central and eastern tropical Pacific; sea surface temperatures (SSTs) in the cold tongue region are warmed (cooled) during El Niño (La Niña) due to a deepening (shoaling) of the eastern tropical Pacific thermocline (Wang et al. 2017). During the boreal winter, the Madden – Julian Oscillation (MJO) is the predominant tropical intraseasonal oscillation (Zhang 2005). The MJO consists of an envelope of alternating enhanced and suppressed convective activity originating in the Indian Ocean and propagating eastward across the western Pacific. In the enhanced convective phase, winds converge at the surface and diverge at the top of the atmosphere. This wind pattern is reversed in the suppressed convective phase. MJO convective activity results in anomalous westerly surface winds in the western Pacific (Hendon et al. 2007) driven by two cyclonic systems located to the north and south of equatorial convection (Rui & Wang, 1990).

Empirical evidence suggests the existence of a sporadic relationship between MJO and ENSO (e.g. Slingo et al. 1999; Hendon et al. 1999; Kessler 2001), despite MJO being a component involved in some ENSO theories. ENSO is described as a self-sustained oscillatory mode for which atmospheric forcing provides the observed regularity and aperiodicity (Battisti 1988; Jin 1997, Kirtman 1997, Neelin et al. 1998; Suarez and Schopf 1988) and/or a damped process for which atmospheric forcing provides the trigger for each discrete event (Lau 1985; Flugel and Chang 1996; Flugel et al. 2004; Kleeman and Moore 1997; Moore and Kleeman 1999a,b; Penland and Matrasova 1994; Penland and Sardeshmukh 1995; Thompson and Battisti 2000, 2001). Theoretical frameworks explaining and quantifying the observed MJO-ENSO relationship are still emerging. The scarcity of theories can be attributed to climate models' deficiency in simulating the MJO and a short record of high-resolution spatial and temporal observations. The record length of observations is not enough to establish robust statistics of ENSO events linked to the MJO and ENSO events not linked to the MJO activity.

Recently, Lybarger and Stan (2018, 2019) and Lybarger et al. (2020) developed an energetic framework that can be applied to quantify the interaction between the MJO and ENSO, providing a coupled ocean-atmosphere perspective consistent with current ENSO theories. Using this framework, Lybarger and Stan (2019) showed that the relative phasing between the MJO and oceanic Kelvin wave activity is the most important factor governing the influence of MJO on ENSO. When in phase and collocated with oceanic Kelvin wave activity, MJO-associated westerly wind stress contributes to the amplification of preexisting downwelling Kelvin waves, leading to earlier onset and greater strength of resulting El Niño events. MJO contributes to the Bjerknes feedback through modulation of the upwelling by thermocline depth anomalies. The out-of-phase interactions between MJO and oceanic Kelvin waves lead to the lack of influence of MJO onto some El Niño events and may be linked to the failure of El Niño initiation. They show that the interaction between MJO activity and Kelvin wave activity is characterized by the MJO wind power measured by the co-variability of MJO-related wind stress and oceanic Kelvin wave activity.

The objective of the project was to adapt the MJO-ENSO diagnostic tool implemented in METplus based on observations to forecast data. Evaluation of the MJO-ENSO interaction in the NOAA UFS model is part of the research being conducted by Loren Doyle as part of her master's thesis work.

Datasets

UFS prototypes (https://registry.opendata.aws/noaa-ufs-s2s/) provide the deterministic reforecast for April 2011 – March 2018. The reforecasts are initialized on the first and fifteenth of each month (168 reforecasts for the entire period) and provide 6-hourly forecasts out to 35 days. The UFS model consists of an atmospheric component (FV3GFS), an oceanic component (GFDL MOM6 model, Adcroft et al. 2019), a sea-ice component (Los Alamos CICE6 model) with a tripolar 0.25^0 global grid and a component for sea waves (WAVEWATCH III; WW3DG, 2019). The coupling of the wave model with the other components is through the National Unified Operational Prediction Capability (NUOPC) component connector. The atmosphere, ocean, and sea-ice models are coupled via the Community Mediator for the Earth Prediction Systems (CMEPS). This is the first UFS prototype using CMEPS for performing custom coupling operations. FV3GFS uses the FV3 dynamical core on the cubed-sphere grid (Putman and Lin, 2007; Harris and Lin, 2013) and the Common Community Physics Package (CCPP) for physics parameterizations. The atmospheric component has a horizontal resolution of ~0.25^0 (C384) and 64 levels in the vertical. The horizontal resolution of the ocean and sea-ice models is 0.25^0.

The MJO-ENSO diagnostic requires five variables: sea surface temperature (SST), zonal and meridional components of the wind stress (τ_x, τ_y) and zonal and meridional components of the ocean surface currents (u, v) in the tropical Pacific domain (15 S – 15 N, 130 E – 85 W). A schematic of the analysis domain is shown in Fig. 1. Note that the land areas in the western Pacific Ocean (e.g. Philippines, Indonesia) are excluded from the calculation.

Figure 1 Tropical Pacific domain used in the calculation of MJO-ENSO diagnostic.

Methodology

All variables required for the calculation of MJO-ENSO diagnostics need pre-processing steps that include computation of daily anomalies defined as deviation from daily climatology across all years. Ingestion of such large datasets is atypical for METplus and the pre-processing step was completed outside of the use case. If regridding of provided anomalies is necessary, the regridding can be completed in METplus.

For UFS, each forecast experiment consisting of 35 days is read in a loop over all years and the diagnostic is computed for each month.

The use case consists of three code components: METcalcpy that contains the Python code calculating the diagnostic, METplotpy that contains Python code for plotting, and METplus wrappers that contains the driver of the calculation, also written in Python, and the configuration script which can be customized to meet the user requirements.

Results

The MJO-ENSO diagnostic consists of two indices derived from the covariability between the MJO component of the wind stress, Kelvin wave activity in the ocean, and SST anomalies associated with El Niño, the *MaKE* and *MaKI* indices (Lybarger et al. 2020). The *MaKE* index is constructed as a predictor of El Niño events; a value of the index greater than -0.5 standard deviation indicates development of SST anomalies that are more likely to result in El Niño. The *MaKI* index is intended as a predictor of El Niño events influenced by the MJO activity; a value of the index smaller than -2 standard deviation indicates development of an El Niño event that is more likely to be influenced by the MJO activity. These threshold values apply mostly to April conditions.

The reforecast period covered by UFS prototypes contains only one El Niño event, which took place in winter 2015/2016, and this event is predicted by the model. Comparison of the SST anomalies evolution corresponding to this event (Fig. 3a) with the SST anomalies evolution of El Niño events observed to interact (Fig. 2a) and not interact (Fig. 2b) with MJO activity suggest no interaction between the MJO activity and the El Niño event. As a result, the UFS reforecast is expected not to predict an El Niño event that is influenced by the MJO activity.

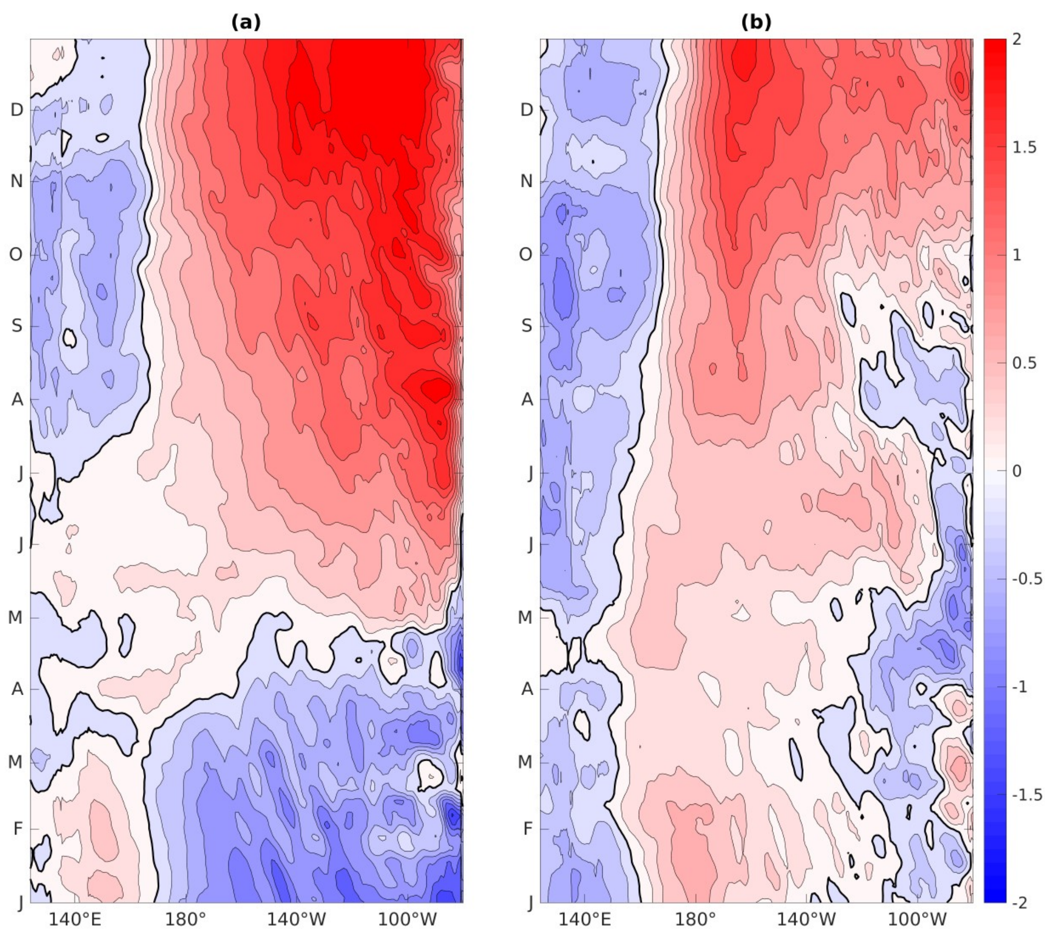

Figure 2 Composites of Hovmöller diagram of equatorially averaged (5S – 5N) SST anomalies for El Niño events which are most influenced by the MJO (a; 1997, 2006, and 2009) and El Niño events which are least influenced by the MJO (b; 1991, 1994, and 2014). Units: °C

For the El Niño event in 2015/2016, the UFS model accurately forecasts SST anomalies (Fig. 3b) corresponding to an oceanic event that is not influenced by the MJO component of the wind stress.

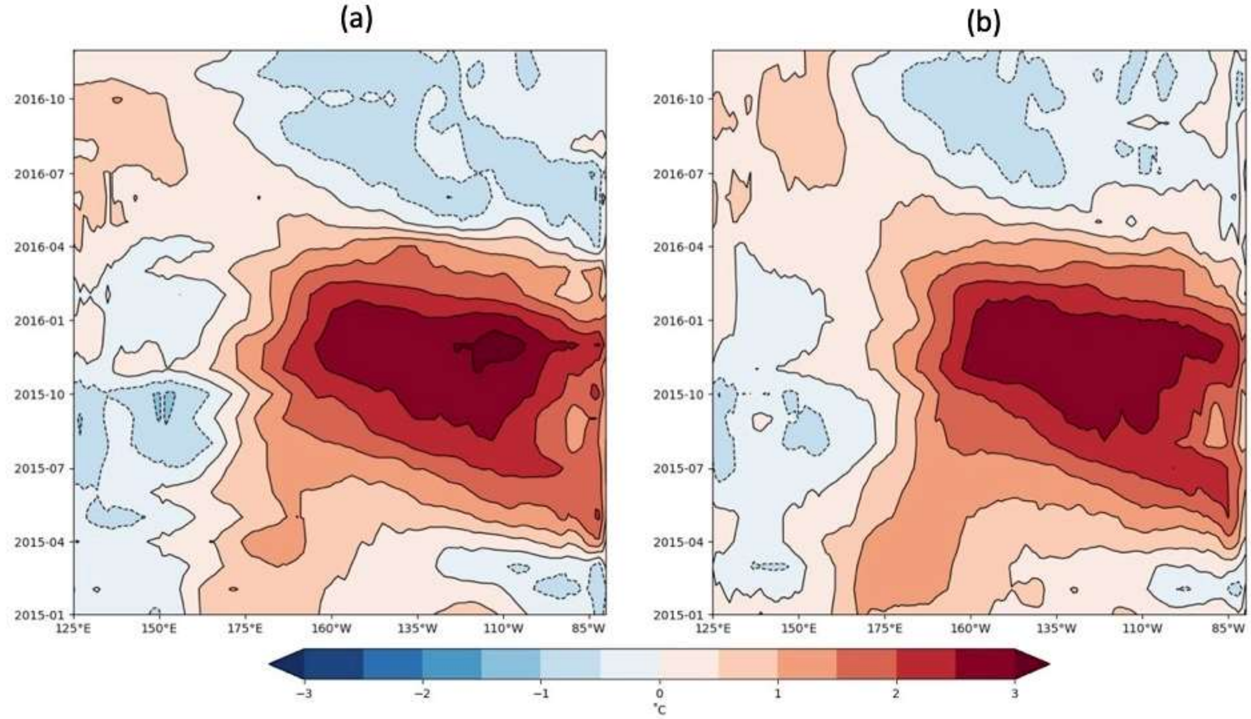

Figure 3 Hovmöller diagram of equatorially averaged (5S – 5N) SST anomalies for El Niño event in 2015/2016 forecasted by UFS (a) and CFS Reanalysis ~~CFSR~~ (b).

Accordingly, the *MaKE* and *MaKI* indices predict an El Niño event with the observed amplitude (Fig. 4a) and not being influenced by the westerly winds associated with the MJO activity (Fig. 4b).

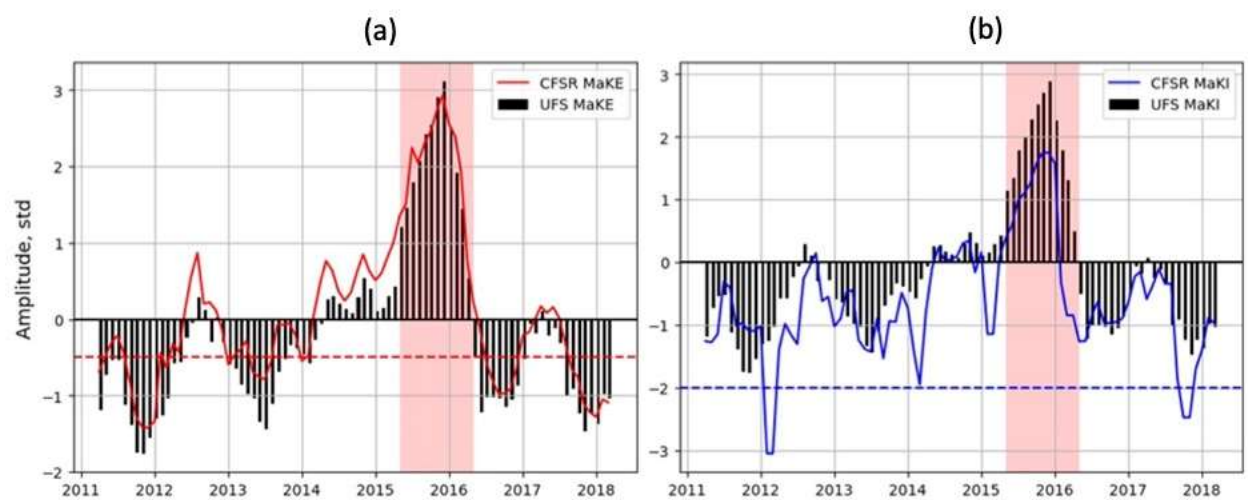

Figure 4 Time series of MaKE (a) and MaKI (b) indices based on CFSR (line) and UFS (bar). The dashed line denotes the index threshold (-0.5 sdt for MaKE) and (-2 std for MaKI). The red background shading marks the El Niño year.

The magnitude of *MaKI* index is slightly higher than in reanalysis. This result suggests that MJO winds project too strongly onto the ocean state during ENSO events.

Future Work

The current code does not support calculation of the MJO-ENSO indices for forecast data consisting of multiple ensemble members. The use case can be applied to the ensemble mean of the forecasts. Future developments will include calculations for individual ensemble members that can then be combined with some of the statistical tools available in METplus such as probability (e.g., HSS, ROC) and ensemble (Rank histogram) scores.

Acknowledgements

Special thanks to Tara Jensen, Christina (Tina) Kalb, Hank Fisher, Minna Win-Gildenmeister, John Opatz, Daniel (Dan) Adriaansen for teaching Loren the development aspects of METplus, the helpful advice with script developments, and the patience in answering our questions.

We are grateful to Tara Jensen and Louisa Nance for the opportunity and experience. We appreciate the efforts of DTC in organizing and hosting our visits.

References

Adcrodft, A., W. G. Anderson, W. G., Balaji, V., Blanton, C., Bushuk, M., Dufour, C. O., Dunne, J. P., Griffies, S. M., Hallberg, R., Harrison, M. J., Held, I. M., Jansen, M., John, J. G., Krasting, J. P., Langenhorst, A. R., Legg, S., Liang, Z., McHugh, C., Radhakrishnan, A., Reichl, B. G., Rosati, A., Samuels, B. L., Shao, A., Stouffer, R. J., Winton, M., Wittenberg, A., Xiang, B., Zadeh, N. & Zhang, R. (2019) The GFDL global ocean and sea ice model OM4.0: Model description and simulation features. *Journal of Advances in Modeling Earth Systems*, **11**. doi:https://doi.org/10.1029/2019MS001726

Battisti, D. (1988) Dynamics and thermodynamics of a warming event in a coupled tropical atmosphere ocean model. *Journal of the Atmospheric Sciences,* **45**, 2889–2919. https://doi.org/10.1175/1520-0469(1988)045<2889:DATOAW>2.0.CO;2

Flugel M., & Chang, P. (1996) Impact of dynamical and stochastic processes on the predictability of ENSO. *Geophysical Research Letters*, **23**, 2089-2092. https://doi.org/10.1029/96GL01959

Flugel M, Chang P, Penland C (2004) The role of stochastic forcing in modulating ENSO predictability. *Journal of Climate*, **17**, 3125–3140. https://doi.org/10.1175/1520-0442(2004)017%3c3125:TROSFI%3e2.0.CO;2

Harris, L. M. & Lin, S.-J. (2013) A two way nested global-regional dynamical core on the cubed-sphere grid. *Monthly Weather Review*, **141**, 283-306. doi:10.1175/MWR-D-11-00201.1

Hendon, H. H., Zhang, C. D., & Glick, J. D. (1999) Interannual variation of the Madden-Julian oscillation during austral summer. *Journal of Climate*, **12**, 2538–2550, https://doi.org/10.1175/1520-0442(1999)012<2538:IVOTMJ>2.0.CO;2.

Hendon, H. H., Wheeler, M. C., & Zhang C. (2007) Seasonal dependence of the MJO–ENSO relationship. *Journal of Climate*, **20**, 531–543.

Jin, F. F. (1997) An equatorial ocean recharge paradigm for ENSO. 1. Conceptual model. *Journal of the Atmospheric Sciences*, **54**, 811–829. https://doi.org/10.1175/1520-0469(1997)054%3c0811:AEORPF%3e2.0.CO;2

Kessler, W. S., (2001) EOF representations of the Madden-Julian oscillation and its connection with ENSO. *Journal of Climate*, **14**, 3055–3061, https://doi.org/10.1175/1520-0442(2001)014<3055:EROTMJ>2.0.CO;2

Kirtman, B. P. (1997) Oceanic Rossby wave dynamics and the ENSO period in a coupled model. *Journal of Climate*, **10**, 1690–1704. https://doi.org/10.1175/1520-0442(1997)010%3c1690:ORWDAT%3e2.0.CO;2

Kleeman, R., Moore, A. M. (1997) A theory for the limitation of ENSO predictability due to stochastic atmospheric transients. *Journal of the Atmospheric Sciences*, **54**, 753–767. https://doi.org/10.1175/1520-0469(1997)054%3c0753:ATFTLO%3e2.0.CO;2

Lau, N.-C. L (1985) Modeling seasonal dependence of the atmospheric response to observed El Ninos in 1962-76. Monthly Weather Review, 113, 1970-1976. https://doi.org/10.1175/1520-0493(1985)113<1970:mtsdot>2.0.CO;2

Lybarger, N. D., & Stan, C. (2018) The effect of the MJO on the energetics of El Niño. *Climate Dynamics*, **51**, 2925–2839, https://doi.org/10.1007/s00382-017-4047-5.

Lybarger, N. D. & Stan, C. (2019) Revisiting MJO, Kelvin waves, and El Niño relationships using a simple ocean model. *Climate Dynamics*, **53**, 6363-6377, https://doi.org/10.1007/s00382-019-04936-5

Lybarger, N. D, Shin, C. -S., & Stan, C. (2020) An MJO wind energy metric for the prediction of El Nino, *Journal of Geophysical Research - Oceans*, **125**, e2020JC016732. https://doi.org/10.1029/2020JC016732

Moore A. M., Kleeman, R. (1999a) Stochastic forcing of ENSO by the intraseasonal oscillation. *Journal of Climate*, **12**, 1199–1220

Moore A. M., Kleeman, R. (1999b) The nonnormal nature of El Niño and intraseasonal variability. *Journal of Climate*, **12**, 2965–2982. https://doi.org/10.1175/1520-0442(1999)012%3c2965:TNNOEN%3e2.0.CO;2

Neelin, J. D., Battisti, D.S., Hirst, A. C., Jin, F. F., Wakamata, Y., Yamagata, T., & Zebiak, S. K. (1998) ENSO theory. *Journal of Geophysical Research-Oceans*, **103**, 14261-14290. https://doi.org/10.1029/97JC03424.

Penland, C., & Matrasova, L. (1994) A balanced condition for stochastic numerical models with applications to El Niño-Southern Oscillation. *Journal of Climate*, **7**, 1352-1372. https://doi.org/10.1175/1520-0442(1994)007<1352:ABCFSN>2.0.CO;2

Penland, C. & Sardeshmukh, P. (1995) The optimal growth of tropical sea surface temperature anomalies. *Journal of Climate*, **8**, 1999-2004. https://doi.org/10.1175/1520-044(1995)008<1999:TOGOTS>2.0CO;2

Putman, W. M., & Lin, S. -J. (2007) Finite-volume transport on various cubed-sphere grids. Journal of *Computational Phys*ics, **227**, 55-78. doi:10.1016/j.jcp.2007.07.022

Rui, H. & Wang, B. (1990) Development characteristics and dynamic structure of tropical intraseasonal convection anomalies. *Journal of the Atmospheric Sciences*, **47**, 357–379.

Slingo, J. M., Rowell, D. P., Sperber, K. R., & Nortley, F. (1999) On the predictability of the interannual behaviour of the Madden-Julian Oscillation and its relationship with El Niño. *Quarterly Journal of the Royal Meteorological Society*, **125**, 583-609.

Suarez, M., & Schopf, P. (1988) A delayed action oscillator for ENSO. *Journal of the Atmospheric Sciences*, **45**, 3283–3287. https://doi.org/10.1175/1520-0469(1988)045%3c3283:ADAOFE%3e2.0.CO;2

The WAVEWATCH III® Development Group (WW3DG), 2019: Use manual and system documentation of WAVEWATCH III® version 6.07. Tech. Note 333, NOAA/NWS/NCEP/MMAB, College Park, MD, USA 465 pp. + App. https://github.com/NOAA-EMC/WW3/wiki/Manual

Thompson, C. J. & Battisti, D. S. (2000) A linear stochastic dynamical model of ENSO. Part I: Model Development. *Journal of Climate*, **13**, 2818-2832. https://doi.org/10.1175/1520-0442(2000)013<2818:ALSDMO>2.0CO;2

Thompson, C. J. & Battisti, D. S. (2001) A linear stochastic dynamical model of ENSO. Part II: Analysis. *Journal of Climate*, **14**, 445-466. https://doi.org/10.1175/1520-0442(2001)014<0445:ALSDMO>2.0CO;2

Wang, C., Deser, C., Yu, J-Y, DiNezio, P., & Clement, A. (2017). El Niño and Southern Oscillation (ENSO): A Review. *Coral Reefs of the Eastern Tropical Pacific*, P.W. Glynn, D. P. Manzello, and I. C. Enochs, Eds., Vol. 8 of, Springer Netherlands, 85–106.

Zhang, C. (2005). Madden-Julian Oscillation. *Review of Geophysics*, **43**, https://doi.org/10.1029/2004RG000158